Available online at www.sciencedirect.com

ScienceDirect

IFAC PapersOnLine 53-1 (2020) 195–200

New tuning strategy for series cascade control structure

Md. Imran Kalim * **Ahmad Ali** **

* *Department of Electrical Engineering, Indian Institute of Technology Patna, Bihta-801106 India (e-mail: imran2025kalim@rediffmail.com).*
** *Department of Electrical Engineering, Indian Institute of Technology Patna, Bihta-801106 India (e-mail: ali@iitp.ac.in).*

Abstract: In the presence of disturbances associated with the manipulated variable, performance of a single loop control structure can be improved with the help of a series cascade control. A design approach for a series cascade control system is proposed in this paper. The secondary controller is tuned by finding the centroid of the convex stability region to quickly attenuate the disturbances arising in the inner loop before they influence the controlled variable, whereas the primary controller is tuned by magnitude optimum criterion to achieve improved servo response in the outer loop. Servo and regulatory responses for the nominal model, as well as for the perturbed model of the plant obtained by the proposed method are compared with some recently reported tuning strategies. Simulation results show that the proposed tuning strategy yields improved closed-loop performance.

Keywords: Cascade control, PID controller, All stabilizing controller, Magnitude optimum criterion.

1. INTRODUCTION

In conventional single loop control structure, disturbance rejection does not take place until the system's output deviates from the set-point. That is why Franks and Worley proposed a cascade control scheme (Franks and Worley (1956)). Fig. 1 shows the block diagram of a series cascade control scheme. $G_{p1}(s)$ and $G_{p2}(s)$ are the transfer functions of primary and secondary processes whereas primary and secondary controllers are represented by $G_{c1}(s)$ and $G_{c2}(s)$ respectively. $y_1(s)$ denotes the output of the outer loop and output of inner loop is represented by $y_2(s)$. Set-point for the outer loop is denoted by $r_1(s)$ whereas output of $G_{c1}(s)$ serves as the set-point (i.e. $r_2(s)$) for the inner loop. $u(s)$ is the manipulated variable. $d_1(s)$ and $d_2(s)$ are the load disturbances entering the outputs of $G_{p1}(s)$ and $G_{p2}(s)$ with disturbance transfer functions $G_{d1}(s)$ and $G_{d2}(s)$ respectively. Series cascade control scheme is used when the dynamics of the inner loop is fast so that there will be rapid attenuation of disturbances in the inner loop. Tuning methods reported for single loop control system, e.g. optimal integral error method (Krishnaswamy et al. (1990)), IMC based tuning method (Lee et al. (2002)), direct synthesis approach (Raja and Ali (2015)) etc. have been extended to cascade control scheme. There exists two different ways to design a cascade control structure. The usual approach is to first tune the secondary controller by assuming the primary controller in open state. The next step is to tune the primary controller with the application of the previously tuned secondary controller to the inner loop. This approach is known as sequential approach. Direct synthesis approach has been used to design the controller settings in Raja and Ali (2015). In Vivek and Chidambaram (2013), a typical relay feedback based autotuning has been applied to the two loops sequentially. Another way of design is simultaneous tuning approach in which the two controllers are tuned concurrently. In Jeng (2014), the controllers are tuned using step response data without considering the process model. The aim is to obtain the controller parameters such that the two loops behave as close as possible to the assumed reference models for the two loops. In Veronesi and Visioli (2011), parameters of the primary and secondary processes were first estimated by evaluating a step response of the system with roughly tuned PID controllers. Then using the estimated model, the two controllers have been tuned by using internal model control strategy. Simultaneous tuning based on user defined settling time and maximum overshoot using genetic algorithm is reported in Kaya and Nalbantoğlu (2016). Internal model control approach was used to simultaneously tune primary and secondary controllers in Jeng and Lee (2012). Two degree of freedom cascade control structures have also been proposed in Alfaro et al. (2008),Alfaro et al. (2009). If there exists a large time delay in the outer loop, a series cascade control structure fails to give acceptable servo and regulatory performances. An improved cascade control structure which uses an internal model control for the inner loop and a PI-PD Smith predictor in the outer loop has been proposed in Kaya et al. (2007) for such class of processes.

Determination of all stabilizing PI, PD and PID controller parameters is reported in Ho et al. (1997); Tan et al. (2003, 2005a, 2006); Onat (2013, 2019). By using the above reported techniques, a convex stability region is obtained inside the stability boundary locus in the plane of controller parameters. Weighted geometrical center (WGC) method and calculation of centroid from the convex stability region has been reported in Onat (2013) and Onat (2019)

2405-8963 © 2020, IFAC (International Federation of Automatic Control) Hosting by Elsevier Ltd. All rights reserved.
Peer review under responsibility of International Federation of Automatic Control.
10.1016/j.ifacol.2020.06.033

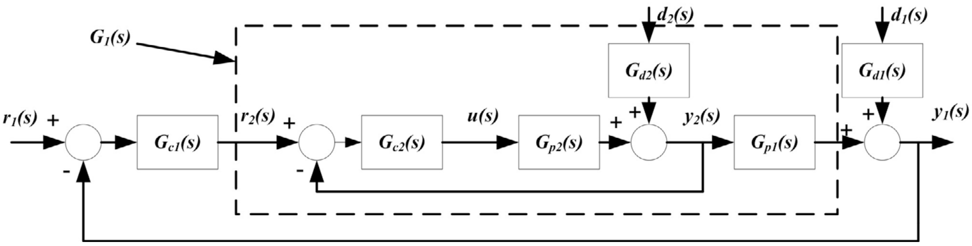

Fig. 1. Series cascade control scheme

respectively. Calculation of WGC is very tedious as it uses all frequency points forming the stability boundary locus, whereas calculation of centroid requires only few frequency dependent points, namely cusp and corner points. It is also reported in Onat (2019) that the controller parameters corresponding to the centroid yields satisfactory closed-loop performance. Furthermore, the centroid is located at a safe distance from all the points on the stability boundary locus. Hence, it will give improved set-point tracking and yields faster disturbance rejection. Also, it will maintain excellent robustness in case of process parameter variations. Hence, the controller settings for the inner loop is obtained by finding the centroid of the convex stability region.

For the output to exactly follow the set point, the closed loop response should have infinite bandwidth and zero phase shift which is practically not possible (Vrancic et al. (2001)). The magnitude optimum criterion tries to maintain the closed loop magnitude frequency response curve flat and close to unity over the widest possible frequency range for any given plant and controller structure (Umland and Safiuddin (1988)). This method is called as modulus optimum (Åström and Hägglund (1995)), Betragsoptimum (Kessler (1955)), magnitude optimum (Umland and Safiuddin (1988)). Actually, this criterion is based on optimizing the closed-loop amplitude response. Furthermore, it is reported in the literature that the magnitude optimum criterion results in superior tracking performance for a large number of process models (Kessler (1955); Vrancic et al. (2001); Vrančić et al. (1999)). Hence, in this proposed work, the primary controller is tuned with the help of magnitude optimum criterion to achieve improved set-point tracking performance and faster disturbance rejection in the outer loop.

The paper is organized as follows: Tuning rules of primary and secondary controllers are derived in Section 2. Simulation examples, results and comparisons are given in Section 3 while Section 4 provides the concluding remarks about the proposed work.

2. TUNING OF G_{C1} AND G_{C2}

2.1 All stabilizing PI controller for G_{c2}

In the proposed work, G_{c2} is considered as a PI controller whose transfer function is given below,

$$G_{c2}(s) = \frac{N_{c2}(s)}{D_{c2}(s)} = K_{p2} + \frac{K_{i2}}{s} \tag{1}$$

where K_{p2} and K_{i2} are the proportional and integral gains of the secondary controller respectively. $G_{c2}(s)$ is tuned by finding the centroid of the convex stability region obtained by plotting the stability boundary locus in K_{p2} and K_{i2} plane (Tan et al. (2003), Onat (2019)). Let, the transfer function of the secondary process be,

$$G_{p2}(s) = \frac{N_{p2}(s)}{D_{p2}(s)} e^{-\tau_2 s} \tag{2}$$

The characteristic polynomial of the inner loop is given by,

$$\begin{aligned} \Delta P(s) &= 1 + G_{c2}(s)G_{p2}(s) \\ &= D_{p2}(s)D_{c2}(s) + N_{p2}(s)N_{c2}(s)e^{-\tau_2 s} \end{aligned} \tag{3}$$

Substituting $s = jw$ and $e^{-\tau_2 s} = e^{-j\tau_2 w} = (cos(\tau_2 w) - jsin(\tau_2 w))$ in (3), we get

$$\begin{aligned} \Delta P(jw) &= D_{p2}(jw)D_{c2}(jw) \\ &\quad + N_{p2}(jw)N_{c2}(jw)(cos(\tau_2 w) - jsin(\tau_2 w)) \end{aligned} \tag{4}$$

Let $R_{\Delta P}$ and $I_{\Delta P}$ represent the real and imaginary parts of $\Delta P(jw)$. Following are the three different ways in which a root of any stable polynomial can cross the imaginary axis (Tan (2009)).

(i) Real Root Boundary (RRB): A real root can cross the imaginary axis at $s = 0$. RRB is obtained by substituting $s = 0$ in (3) which gives $K_{i2} = 0$ as the RRB line.

(ii) Infinite Root Boundary (IRB): A real root can cross the imaginary axis at $s = \infty$. IRB is obtained by substituting $s = \infty$ in (3). There will not be any IRB line for proper transfer function.

(iii) Complex Root Boundary (CRB): Roots on the imaginary axis can become unstable which implies that both the real and imaginary parts of (4) will become zero simultaneously.

The procedure to obtain complex root boundary is given in Tan (2009) and is discussed below in brief.

K_{p2} and K_{i2} are obtained as functions of w by solving $R_{\Delta P} = 0$ and $I_{\Delta P} = 0$. The complex root boundary in K_{p2} and K_{i2} plane is obtained by varying w from 0 to w_c, where w_c is the lowest value of frequency other than $w = 0$ at which $K_{i2} = 0$. Convex stability region in K_{p2} and K_{i2} plane is the area bounded by CRB and RRB which contains all the stabilizing values of K_{p2} and K_{i2} for the considered plant. The cusp and corner points of the convex stability region are identified as $(K'_{p1}, K'_{i1}), (K'_{p2}, K'_{i2}) \ldots\ldots (K'_{pm}, K'_{im})$ and $(K''_{p1}, K''_{i1}), (K''_{p2}, K''_{i2}) \ldots\ldots (K''_{pn}, K''_{in})$, where m and n are the number of cusp and corner points respectively. The parameters of inner controller are obtained by finding the centroid of the convex stability region as given below (Onat (2019)),

$$K_{p2} = \frac{(\sum_{l=1}^{m} K'_{pl}) + (\sum_{l=1}^{n} (K''_{pl})}{m+n} \tag{5}$$

$$K_{i2} = \frac{(\sum_{l=1}^{m} K'_{il}) + (\sum_{l=1}^{n} (K''_{il})}{m+n} \tag{6}$$

2.2 Magnitude optimum criterion for G_{c1}

In the proposed work, $G_{c1}(s)$ is assumed as a PID controller with following transfer function:

$$G_{c1}(s) = K_{p1} + \frac{K_{i1}}{s} + K_{d1}s \tag{7}$$

where K_{p1}, K_{i1} and K_{d1} are the proportional, integral and derivative gains of the primary controller respectively. From Fig. 1, $G_1(s)$ can be calculated as,

$$G_1(s) = \frac{G_{c2}(s)G_{p2}(s)}{1 + G_{c2}(s)G_{p2}(s)}G_{p1}(s) \tag{8}$$

.Let $G_{cl}(s)$ be the closed loop transfer function from reference to output. To achieve the magnitude optimum criterion, the controller should satisfy the following two conditions for as many q as possible (Vrancic et al. (2001)):

$$G_{cl}(0) = 1 \tag{9}$$

$$\left.\frac{d^q|G_{cl}(jw)|}{dw^q}\right|_{w=0} = 0, q = 1, 2, ..., q_{max} \tag{10}$$

First equation can be satisfied by using a controller structure having an integral term. q_{max} is taken as 2 for a PI controller and 3 for a PID controller. Assuming that the plant model for the primary controller is given as follows:

$$G_1(s) = K_r\frac{1 + a_1s + a_2s^2 + ... + a_ms^m}{1 + b_1s + b_2s^2 + ... + b_ns^n}e^{-\tau_1 s} \tag{11}$$

where K_r is the process steady state gain, τ_1 is the process time delay. (a_1,..., a_m) and (b_1,..., b_m) are the process parameters. Time delay term is replaced by its Taylor's series approximation. Multiplying (7) and (11), the open loop transfer function becomes,

$$G_1(s)G_{c1}(s) = \frac{c_0 + c_1s + c_2s^2 + ...}{d_0s + d_1s^2 + d_2s^3 + ...} \tag{12}$$

where, the coefficients c_i and d_i $(i = 0, 1, 2, 3...)$ are functions of the plant and controller parameters which can be obtained using the expressions given below (Vrancic et al. (2001)):

$$\begin{aligned} d_i &= b_i \\ c_i &= K_r[K_{i1}\phi_i + K_{p1}\phi_{i-1} + K_{d1}\phi_{i-2}] \end{aligned}$$

$$\phi_i = \sum_{l=0}^{i}(-1)^{i-l}a_l\frac{\tau_1^{i-l}}{(i-l)!}$$

$$a_0 = b_0 = 1$$

$$a_i = b_i = 0, i < 0. \tag{13}$$

Necessary and sufficient condition for stability reported in Hanus (1975) is as given below:

$$\frac{c_0}{d_0} > 0 \tag{14}$$

The PID controller parameters can be obtained by solving the following equations for $n = 0 - 2$ (Hanus (1975)).

$$\sum_{i=0}^{2n+1}(-1)^ic_id_{2n+1-i} = 0.5\sum_{i=0}^{2n}(-1)^id_id_{2n-i} \tag{15}$$

By substituting (13) into (15), following expressions are obtained for K_{p1} , K_{i1} and K_{d1} (Vrancic et al. (2001)).

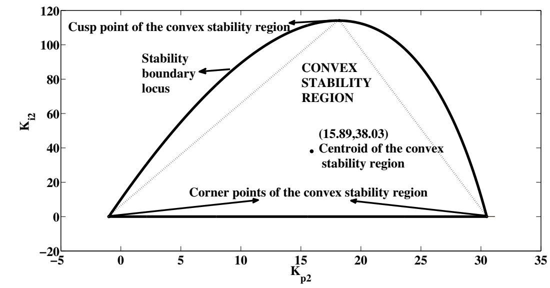

Fig. 2. Stability boundary locus of inner loop of example 1

$$K_{p1} = \frac{A_3^2 - A_1A_5}{2(A_1A_2A_3 + A_0A_1A_5 - A_1^2A_4 - A_0A_3^2)} \tag{16}$$

$$K_{i1} = \frac{A_2A_3 - A_1A_4}{2(A_1A_2A_3 + A_0A_1A_5 - A_1^2A_4 - A_0A_3^2)} \tag{17}$$

$$K_{d1} = \frac{A_3A_4 - A_2A_5}{2(A_1A_2A_3 + A_0A_1A_5 - A_1^2A_4 - A_0A_3^2)} \tag{18}$$

where symbols A_0, A_1, A_2, A_3, A_4 and A_5 are known as characteristic areas of the process. These areas can be calculated using the following expressions.

$$A_0 = K_r$$

$$A_j = K_r\left((-1)^{j+1}(b_j - a_j) + (\sum_{l=1}^{j}(-1)^{j+l}\frac{\tau_1^lb_{j-l}}{l!})\right) + \sum_{l=1}^{j-1}(-1)^{j+l-1}A_la_{j-l} \tag{19}$$

3. SIMULATION EXAMPLES

In this section, three simulation examples are provided to demonstrate the effectiveness of the proposed method. Following commonly used parallel form of PID controller is used in simulation.

$$G_{c1}(s) = K_{p1} + \frac{K_{i1}}{s} + \frac{K_{d1}s}{t_{f1}s + 1} \tag{20}$$

where, $t_{f1} = 0.1T_{d1}$, and $T_{d1} = K_{d1}/K_{p1}$.

Example 1.

In Jeng (2014), following higher order process has been studied.

$$G_{p1}(s) = G_{d1}(s) = \frac{1}{(10s + 1)(4s + 1)(s + 1)^2}$$

$$G_{p2}(s) = G_{d2}(s) = \frac{1}{1.9s + 1}e^{-0.1s} \tag{21}$$

For tuning of secondary controller, convex stability region of the inner loop is obtained in K_{p2} and K_{i2} plane using the procedure given in section 2.1, and is shown in Fig. 2. It is having one cusp point and two corner points as shown. Centroid of the convex stability region is calculated using (5) and (6). By applying (16) to (18), controller settings for outer loop are obtained. Table 1 shows the controller tuning parameters for the method of Jeng (2014) and the proposed technique. Closed loop response to unit step setpoint change at $t = 0s$, step input disturbances $d_2 = 30$ at $t = 80s$ and $d_1 = 1$ at $t = 160s$ is shown in Fig. 3 while control signal is provided in Fig. 4. Performance measures are given in Table 2. To show the robustness to parameter

Table 1. **Controller tuning parameters for various examples.**

	Tuning method	Inner loop		Outer loop		
		K_{p2}	K_{i2}	K_{p1}	K_{i1}	K_{d1}
Example 1	**J.C.Jeng**	3.633	3.043	1.974	0.1376	6.025
	Proposed	15.89	38.03	3.8113	0.2690	11.219
Example 2	**J.C.Jeng**	0.617	0.0595	0.088	0.0010136	2.27304
	Proposed	1.218	0.128	0.1016	0.0012	2.2703
Example 3	**Kaya and Nalbantoglu**	1.2214	1.2214	1	0.32106	0.6090
	Proposed	0.79	5.73	1.0548	0.4897	0.5899

Table 2. **Performance measures for various examples.**

		Servo	Performance	Regulatory(d2)	Performance	Regulatory (d1)	Performance
		J.C.Jeng	Proposed	J.C.Jeng	Proposed	J.C.Jeng	Proposed
	$\mathbf{T_r}$**(sec.)**	10.5	**7.7**	-	-	-	-
	$\mathbf{T_s}$**(sec.)**	21.6	**13.7**	51	**7.8**	50	**38**
Example 1	**%**$\mathbf{M_p}$	**0**	6	38.3	**2.7**	31	**20**
	IAE	7.268	**4.272**	6.064	**0.3149**	7.257	**3.714**
	ISE	4.807	**2.993**	1.164	**0.00485**	1.517	**0.4766**
	ITAE	38.46	**13.01**	121.3	**4.827**	153.8	**66.12**
	$\mathbf{T_r}$**(sec.)**	390	**146.3**	-	-	-	-
	$\mathbf{T_s}$**(sec.)**	**201**	231	425	**334**	408	**317.5**
Example 2	**%**$\mathbf{M_p}$	**0.12**	5.84	53.1	**24.5**	60.7	**57.6**
	IAE	98.95	**91.98**	80.82	**36.01**	98.77	**83.36**
	ISE	75.4	**69.39**	24.98	**5.478**	41.67	**34.51**
	ITAE	6042	**5364**	14990	**6160**	17810	**13790**
		Kaya and Nalbantoglu	Proposed	Kaya and Nalbantoglu	Proposed	Kaya and Nalbantoglu	Proposed
	$\mathbf{T_r}$**(sec.)**	4.64	**2.94**	-	-	-	-
	$\mathbf{T_s}$**(sec.)**	**5.587**	7.1	12.37	**6.72**	14.27	**8.6**
Example 3	**%**$\mathbf{M_p}$	**1.006**	8.1	**16.2**	16.3	63.5	**60.2**
	IAE	3.1298	**2.3**	0.7874	**0.2092**	3.115	**2.047**
	ISE	2.485	**1.82**	0.06688	**0.00817**	1.288	**0.8686**
	ITAE	5.687	**3.318**	5.054	**0.8688**	16.85	**8.273**

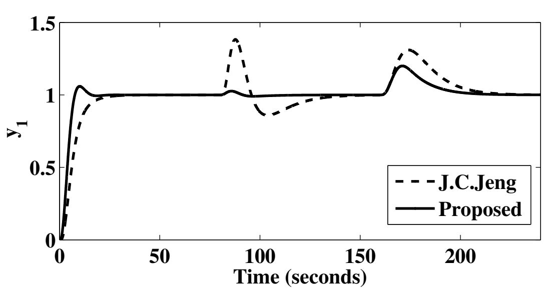

Fig. 3. Closed-loop response of example 1

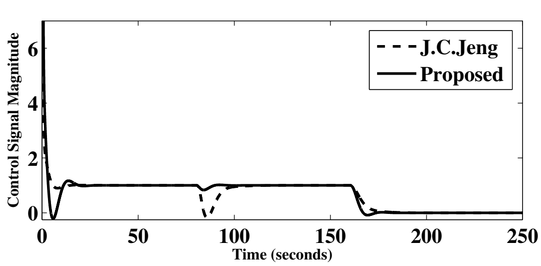

Fig. 4. Control signal of example 1

variations of the plant, the controller is applied to following perturbed model of the plant.

$$G_{p1}(s) = \frac{1.2}{(8s+1)(3.2s+1)(0.8s+1)^2}$$
$$G_{p2}(s) = \frac{1.2}{1.65s+1}e^{-0.12s} \tag{22}$$

Closed loop response for the perturbed plant is shown in Fig. 5. So, the proposed method provides excellent robustness with improved closed loop response. It can be concluded from Fig. 3, Fig. 4, Fig. 5, and Table 2 that the proposed method performs better than the strategy reported in Jeng (2014).

Example 2.

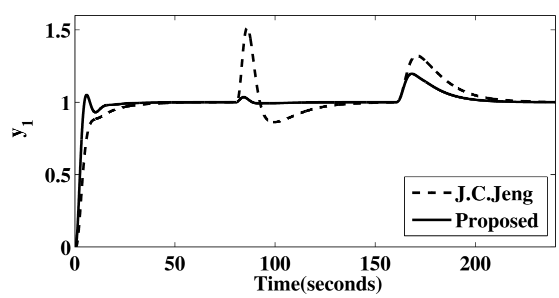

Fig. 5. Closed-loop response for the perturbed plant of example 1

Let us consider the following higher order process which exhibits nonminimum-phase dynamics (Jeng (2014)).

$$G_{p1}(s) = G_{d1}(s) = \frac{10(-5s+1)}{(30s+1)^3(10s+1)^2}e^{-5s}$$
$$G_{p2}(s) = G_{d2}(s) = \frac{3}{13.3s+1}e^{-3s} \tag{23}$$

The computed convex stability region is shown in Fig. 6.

Table 1 summarizes the controller settings for the inner and outer loops for the design method of Jeng (2014) and the proposed technique. Fig. 7 shows the closed loop response to unit step set point change at $t = 0s$, step input disturbances $d_2 = 0.4$ at $t = 700s$ and $d_1 = 0.1$ at $t = 1400s$. Control signal is shown in Fig. 8. For robustness consideration, following perturbed model of the plant has been considered.

$$G_{p1}(s) = \frac{12(-6s+1)}{(24s+1)^3(8s+1)^2}e^{-6s}$$
$$G_{p2}(s) = \frac{3.6}{10.64s+1}e^{-3.6s} \tag{24}$$

It is observed from Fig. 7, Fig. 8, Fig. 9, and Table 2 that the proposed method yields improved closed loop

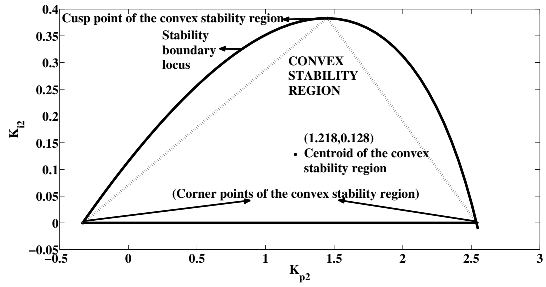

Fig. 6. Stability boundary locus of inner loop of example 2

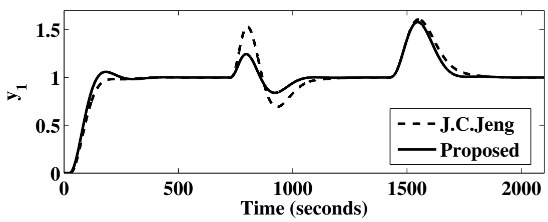

Fig. 7. Closed-loop response of example 2

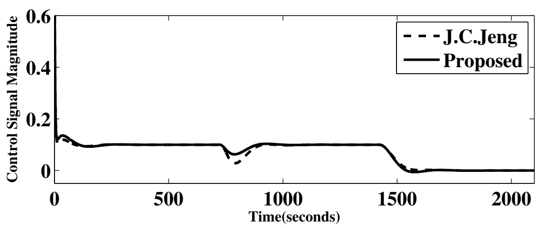

Fig. 8. Control signal of example 2

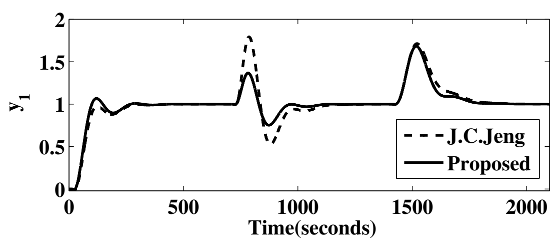

Fig. 9. Closed-loop response for the perturbed plant of example 2

performance for nominal as well as perturbed model of the plant.

Example 3.
As a third example, Following self regulating process has been considered (Kaya and Nalbantoğlu (2016)).

$$G_{p1}(s) = G_{d1}(s) = \frac{1}{(s+1)^2}e^{-s}$$
$$G_{p2}(s) = G_{d2}(s) = \frac{1}{0.1s+1}e^{-0.1s} \tag{25}$$

The convex stability region is shown in Fig. 10. Obtained values of the controller parameters for the two loops are given in Table 1 for the proposed method and the design approach of Kaya and Nalbantoğlu (2016) . Fig. 11 shows the closed loop response to unit step set-point change at $t = 0s$, step input disturbances $d_2 = 1$ at $t = 40s$ and

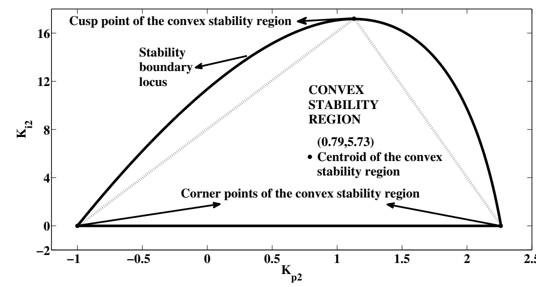

Fig. 10. Stability boundary locus of inner loop of example 3

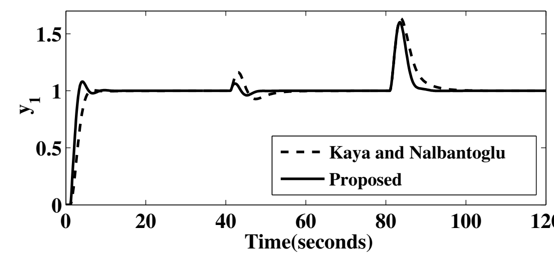

Fig. 11. Closed-loop response of example 3

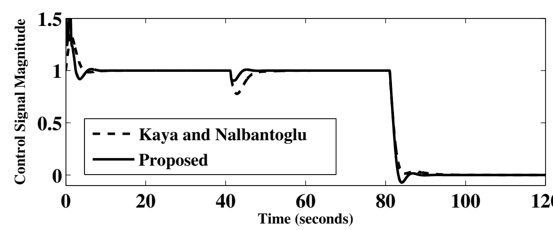

Fig. 12. Control signal of example 3

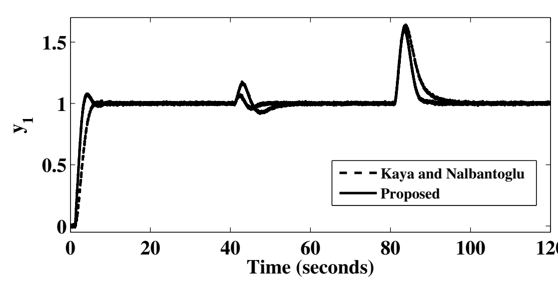

Fig. 13. Closed-loop response under noise for example 3

$d_1 = 1$ at $t = 80s$. Control signal is provided in Fig. 12. As can be seen from the graph that the proposed method yields improved servo as well as regulatory responses as compared to the method of Kaya and Nalbantoğlu (2016). To demonstrate the effects of the noise constraint, the system is subjected to white noise of standard deviation $\sigma_n = 0.005$, band-limited by the Nyquist frequency corresponding to the controller sampling period h = 0.01. Closed-loop response and corresponding control signal under noise are shown in Fig. 13 and Fig. 14 respectively. As shown in the figures, the response by the proposed method shows still better performance than that by the method of Kaya and Nalbantoğlu (2016).

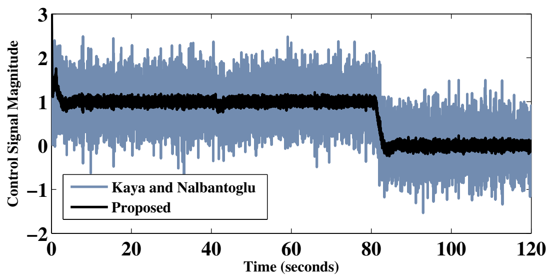

Fig. 14. Control signal under noise for example 3

4. CONCLUSIONS

A tuning strategy for a series cascade control structure has been presented in this paper. Simulation examples have been provided to show the benefits of the proposed technique. Closed-loop responses illustrate that the proposed tuning method yields better servo and regulatory performances as compared to the recently reported tuning strategies for the nominal as well as the perturbed model of the plant. The improved results of the procedure are demonstrated with respect to measurement noise. An extension of the present work can include the simultaneous tuning of series cascade control system and also the incorporation of performance-robustness trade-off into the parameter selection criterion.

REFERENCES

Alfaro, V.M., Vilanova, R., and Arrieta, O. (2008). Two-degree-of-freedom PI/PID tuning approach for smooth control on cascade control systems. In *47th IEEE Conference on Decision and Control*, 5680–5685. IEEE.

Alfaro, V., Vilanova, R., and Arrieta, O. (2009). Robust tuning of two-degree-of-freedom (2-dof) PI/PID based cascade control systems. *Journal of process control*, 19(10), 1658–1670.

Åström, K.J. and Hägglund, T. (1995). *PID controllers: theory, design, and tuning*, volume 2. Instrument society of America Research Triangle Park, NC.

Franks, R. and Worley, C. (1956). Quantitative analysis of cascade control. *Industrial & Engineering Chemistry*, 48(6), 1074–1079.

Hanus, R. (1975). Determination of controllers parameters in the frequency domain. *Journal A*, 16(3), 128.

Ho, M.T., Datta, A., and Bhattacharyya, S. (1997). A linear programming characterization of all stabilizing PID controllers. In *Proceedings of the American Control Conference*, volume 6, 3922–3928. IEEE.

Jeng, J.C. (2014). Simultaneous closed-loop tuning of cascade controllers based directly on set-point step-response data. *Journal of Process Control*, 24(5), 652–662.

Jeng, J.C. and Lee, M.W. (2012). Simultaneous automatic tuning of cascade control systems from closed-loop step response data. *Journal of Process Control*, 22(6), 1020–1033.

Kaya, İ. and Nalbantoğlu, M. (2016). Simultaneous tuning of cascaded controller design using genetic algorithm. *Electrical Engineering*, 98(3), 299–305.

Kaya, I., Tan, N., and Atherton, D.P. (2007). Improved cascade control structure for enhanced performance. *Journal of Process Control*, 17(1), 3–16.

Kessler, C. (1955). Über die vorausberechnung optimal abgestimmter regelkreise teil 111. die optimale einstellung des reglers nach dem betragsoptimum. *Regelmgstechnik*, 40–49.

Krishnaswamy, P.R., Rangaiah, G.P., Jha, R.K., and Deshpande, P.B. (1990). When to use cascade control. *Industrial & engineering chemistry research*, 29(10), 2163–2166.

Lee, Y., Oh, S., and Park, S. (2002). Enhanced control with a general cascade control structure. *Industrial & engineering chemistry research*, 41(11), 2679–2688.

Onat, C. (2013). A new concept on PI design for time delay systems: weighted geometrical center. *International Journal of Innovative Computing, Information and Control*, 9(4), 1539–1556.

Onat, C. (2019). A new design method for PI-PD control of unstable processes with dead time. *ISA Transactions*, 84, 69–81.

Raja, G.L. and Ali, A. (2015). Improved tuning of cascade controllers for stable and integrating processes with time delay. *Michael Faraday IET International Summit, Kolkata, India.*

Tan, N. (2009). Computation of stabilizing PI-PD controllers. *International Journal of Control, Automation and Systems*, 7(2), 175–184.

Tan, N., Kaya, I., and Atherton, D.P. (2003). Computation of stabilizing PI and PID controllers. In *Proceedings of IEEE Conference on Control Applications*, volume 2, 876–881. IEEE.

Tan, N., Kaya, I., and Atherton, D.P. (2005a). A graphical method for computation of all stabilizing PI controllers. *IFAC Proceedings Volumes*, 38(1), 349–354.

Tan, N., Kaya, I., Yeroglu, C., and Atherton, D.P. (2006). Computation of stabilizing PI and PID controllers using the stability boundary locus. *Energy Conversion and Management*, 47(18-19), 3045–3058.

Tan, W., Liu, J., Chen, T., and Marquez, H.J. (2005b). Robust analysis and pid tuning of cascade control systems. *Chemical Engineering Communications*, 192(9), 1204–1220.

Umland, J.W. and Safiuddin, M. (1988). Magnitude and symmetric optimum criterion for the design of linear control systems-what is it and does it compare with the others? In *Conference Record of the IEEE Industry Applications Society Annual Meeting*, 1796–1802. IEEE.

Veronesi, M. and Visioli, A. (2011). Simultaneous closed-loop automatic tuning method for cascade controllers. *IET Control Theory & Applications*, 5(2), 263–270.

Vivek, S. and Chidambaram, M. (2013). Cascade controller tuning by relay auto tune method. *Journal of the Indian Institute of Science*, 84(3 & 4), 89.

Vrančić, D., Peng, Y., and Strmčnik, S. (1999). A new PID controller tuning method based on multiple integrations. *Control Engineering Practice*, 7(5), 623–633.

Vrancic, D., Strmcnik, S., and Jurcic, D. (2001). A magnitude optimum multiple integration tuning method for filtered PID controller. *Automatica*, 37(9), 1473–1479.